Progress In Electromagnetics Research B, Vol. 56, 309–326, 2013

ANALYTICAL EVALUATION OF SUB-SEA ELF ELECTROMAGNETIC FIELD GENERATED BY SUBMARINE POWER CABLES

Giovanni Lucca*

SIRTI S.p.A. Via Stamira d'Ancona 9, Milano 20127, Italy

Abstract—This paper presents analytical formulas, based on the "thin wire model", for calculating the ELF (Extremely Low Frequency) sub-sea electromagnetic field produced by a submarine power cable. Two different models are studied: the first and simpler one (already present in literature) is based on the infinite sea model while the second and more realistic one, that we propose, takes into account of the seabed presence with the sea considered having finite depth. The shielding effect produced by cable sheath and armouring is taken into account by means of suitable shielding factors. Some examples of application of the two models are shown and the relevant results are compared between them.

1. INTRODUCTION

The interest in ELF electromagnetic field generated by submerged cables in conductive media, arose, in the last century, in connection with geophysical exploration and submarine communication/navigation ([1–4]). More recently, a completely different problem stimulated the research concerning sub-sea ELF electromagnetic field; the new motivation is related to the increasing demand of renewable energy that has led to planning and construction of a large number of offshore wind farms especially in the Northern Europe; thus, due to the increasing number of submarine power cables departing from offshore wind farms, concern exists for the potential effect on the marine environment produced by the ELF electromagnetic field (EMF) generated by the cables themselves.

It is worthwhile to just mention the potential effects of the EMF on certain marine organisms [5–7]:

Received 29 August 2013, Accepted 6 November 2013, Scheduled 9 November 2013

* Corresponding author: Giovanni Lucca (G.Lucca@sirti.it).

- Affect orientation.
- Disruption of migrations.
- Attraction/repulsion of animals.
- Egg/larval development impact.

So, EMF is an issue for the offshore renewable energy industry because as a source of potential environmental impact, it is a matter of concern to environmental regulators; moreover, in some countries, it is mandatory to describe such a potential impact as a prerequisite in order to get the necessary authorizations in order to build up new plants. Therefore, it is useful to have at disposal a simulation tool able to assess the level of underwater EMF generated in the space surrounding a submarine power cable.

Previous works concerning the modelling and the calculation of sub-sea EMF generated by submarine power cables are [8, 9]. By using a 2D FEM (Finite Elements Method) technique, the authors discretise, through a suitable mesh, the inner space inside the cable (i.e., phase conductors, insulating material, sheath, armouring) and the outer space (i.e., the sea water and the seabed) and obtain the value of the EMF inside and outside the cable.

A further and more recent approach is the one described in [10] which is based on the concept of radial transmission line model. Such a transmission line comprises concentric shells that are thin compared to both power cable radius and skin depth of a plane wave propagating into the sea that is modelled as an infinite and homogeneous medium. The propagation across each shell is defined by near constant parameters (resistance, inductance, capacitance and conductance) at a specific radius, and they are used to define a radial distributed transmission line model that allows for the calculation of the EMF in the sea.

For our proposal to study the EMF only outside the cable, we would like to propose, in this paper, a methodology which is based on modelling the cable phase conductors by means of *thin wires*. Thus, by starting from the contribution in [4], we have improved the analytical approach there described and based on *infinite sea model*, by modelling the finite depth of the sea and the presence of the seabed with its own resistivity. Hence, from this point of view, the *finite depth sea model* is more realistic than the *infinite sea model*.

Moreover, the shielding effect of metallic cable sheath and armouring is taken into account by means of suitable shielding factors that can be analytically calculated on the basis of cable physical and geometrical characteristics.

The main advantage of such an approach is that analytical

expressions (that can be quickly implemented by means of a computer program) for the EMF in the sea can be found.

2. ANALYTICAL FORMULAS FOR EMF IN THE SEA

2.1. General

As already mentioned, our aim is the EMF calculation only outside the cable; so, we can use the *thin wire approximation* that allows us to treat the phase conductors of the cable as filamentary conductors carrying a known current. That means to neglect phenomena of skin effect and proximity effect for the cable conductors. This assumption is quite reasonable as far as we are interested in calculating the field outside the cable.

The cable conductors are very long so that we can consider them of infinite length. Moreover, especially at the low frequencies considered in this paper, (typically 50–60 Hz) we can neglect current variations along the cable so that the current carried by each conductor can be considered, with good approximation, constant.

Due to the above assumptions, we can adopt a 2D model for the description of the EMF generated around the cable.

On the basis of these simplifying hypotheses, we consider in the next paragraphs two different models:

- A simple model of *infinite* sea, i.e., a wire carrying a known current located inside an infinite, homogeneous and isotropic medium.
- A model of *finite depth sea*, i.e., a wire carrying a known current located at the interface between sea (considered of finite depth) and seabed; thus, this model takes into account of three different media: seabed, sea water and air.

The results obtained by the two models shall be then compared by varying some of the more significant parameters present in the models themselves.

Finally, we have to mention that a further hypothesis adopted in both the models is neglecting, in conductive media, the displacement current with respect to the conduction current. Such an assumption is acceptable when the following equation holds:

$$\frac{1}{\rho_i} \gg \omega\varepsilon_i \quad i = 1, 2 \tag{1}$$

ρ_1 and ε_1 being the sea water resistivity and permittivity, respectively, ρ_2 and ε_2 the corresponding quantities relevant to the seabed, $\omega = 2\pi f$ the angular frequency, and f the frequency.

Note that due to the low frequency considered ($f = 50\,\text{Hz}$–$60\,\text{Hz}$), and inside the typical range of values for resistivity and permittivity relevant to sea water and seabed, inequality (1) is always verified.

2.2. Infinite Sea Model

Let us consider the k-th phase conductor carrying a constant and known current I_k located in an infinite sea (see Figure 1).

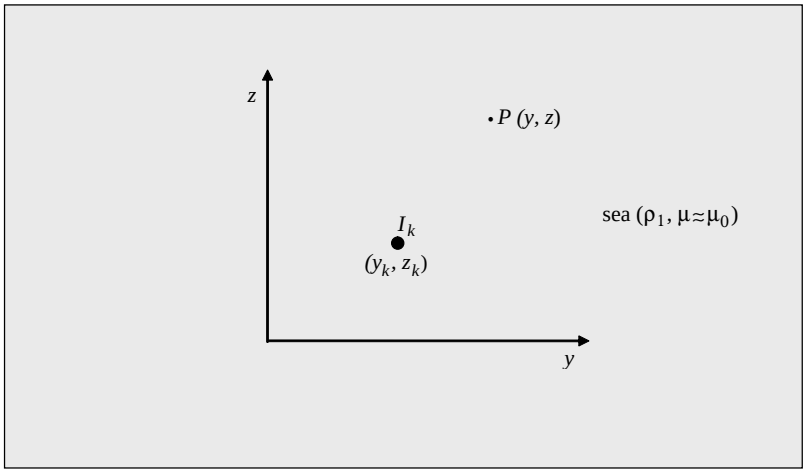

Figure 1. Conductor immersed in an infinite sea.

According to the geometry sketched in Figure 1, the EMF has cylindrical symmetry, and electric and magnetic flux density field components have been deduced in [4].

We report them (in a slightly different form that takes into account also of the cable radius) according the conventions and notations used in Figure 1.

The electric field E in a generic point P of coordinates (y, z) has only the x component which is given by:

$$E_{xk}(y,z) = -\sqrt{\frac{j\omega\mu_0}{\rho_1}}\frac{\rho_1 I_k}{2\pi r_{ck}}\frac{K_0\left(\sqrt{\frac{j\omega\mu_0}{\rho_1}}\sqrt{(y-y_k)^2+(z-z_k)^2}\right)}{K_1\left(\sqrt{\frac{j\omega\mu_0}{\rho_1}}r_{ck}\right)} \quad (2)$$

While the y and z components of the magnetic flux density field B, evaluated in P, are:

$$B_{yk}(y,z) = \frac{\mu_0 I_k}{2\pi\, r_{ck}}\frac{K_1\left(\sqrt{\frac{j\omega\mu_0}{\rho_1}}\sqrt{(y-y_k)^2+(z-z_k)^2}\right)}{K_1\left(\sqrt{\frac{j\omega\mu_0}{\rho_1}}r_{ck}\right)}$$

$$\frac{(y-y_k)}{\sqrt{(y-y_k)^2+(z-z_k)^2}} \tag{3}$$

$$B_{zk}(y,z) = -\frac{\mu_0 I_k}{2\pi\, r_{ck}} \frac{K_1\left(\sqrt{\frac{j\omega\mu_0}{\rho_1}}\sqrt{(y-y_k)^2+(z-z_k)^2}\right)}{K_1\left(\sqrt{\frac{j\omega\mu_0}{\rho_1}}r_{ck}\right)}$$

$$\frac{(z-z_k)}{\sqrt{(y-y_k)^2+(z-z_k)^2}} \tag{4}$$

In formulas (2)–(4), j is the imaginary unit, ρ_1 the sea water resistivity, μ_0 the vacuum permeability, r_{ck} the radius of the k-th conductor, and K_0 and K_1 are the modified Bessel functions of second kind and order 0 and 1, respectively. Moreover, the following condition must hold:

$$\mathrm{Re}\left(\sqrt{\frac{j\omega\mu_0}{\rho_1}}\right) > 0 \tag{5}$$

Lastly, in formulas (2)–(4) when the argument of K_1 at the denominator is very small (condition actually verified in the practice), the expressions for the EMF become identical to the ones reported in [4].

2.3. Finite Depth Sea Model

Let us now propose a more realistic model of sea having depth d with the k-th conductor located at the interface between the sea water and seabed (see the sketch in Figure 2).

The formulas for the EMF that we would like to propose are based on the results presented in [11] where the authors studied the case of a buried cable in a two-layer soil. Here, in the frame of our problem, the first layer plays the role of the sea water while the second layer plays the role of the seabed (note that actually three different media are considered in this model: air, sea water and seabed); thus, by specializing those formulas for the present application, we obtain for the electric field E' and magnetic flux density field B':

$$E'_{xk} = -\frac{j\omega\mu_0 I_k}{2\pi}\int_0^\infty \frac{\cos\lambda\,(y-y_k)}{\alpha_1} \frac{\begin{array}{c} s_{10}s_{21}e^{-\alpha_1|z-z_k|} + s_{10}d_{21}e^{-\alpha_1(z+z_k)} \\ +d_{10}s_{21}e^{-\alpha_1(2d-z-z_k)} + d_{10}d_{21}e^{-\alpha_1(2d-|z-z_k|)} \end{array}}{s_{10}s_{21} - d_{10}d_{21}e^{-2\alpha_1 d}} d\lambda \tag{6}$$

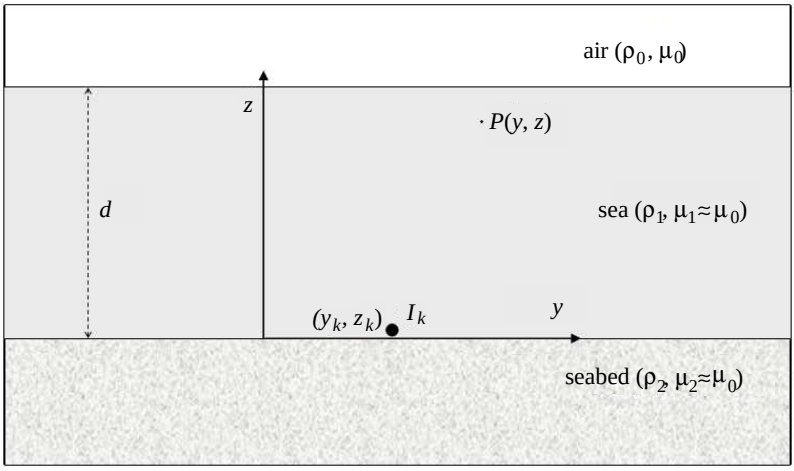

Figure 2. Conductor lying on the seabed and immersed in a finite depth sea.

$$B'_{yk} = \frac{\mu_0 I_k}{2\pi} \int_0^\infty \frac{\begin{array}{c} -\text{sign}\,(z-z_k)\, s_{10} s_{21} e^{-\alpha_1 |z-z_k|} \\ -s_{10} d_{21} e^{-\alpha_1 (z+z_k)} + d_{10} s_{21} e^{-\alpha_1 (2d-z-z_k)} \\ +\,\text{sign}\,(z-z_k)\, d_{10} d_{21} e^{-\alpha_1 (2d-|z-z_k|)} \end{array}}{s_{10} s_{21} - d_{10} d_{21} e^{-2\alpha_1 d}} \cos\lambda\,(y-y_k)\, d\lambda \tag{7}$$

$$B'_{zk} = \frac{\mu_0 I_k}{2\pi} \int_0^\infty \frac{\lambda \sin\lambda\,(y-y_k)}{\alpha_1} \frac{\begin{array}{c} s_{10} s_{21} e^{-\alpha_1 |z-z_k|} + s_{10} d_{21} e^{-\alpha_1 (z+z_k)} \\ +d_{10} s_{21} e^{-\alpha_1 (2d-z-z_k)} + d_{10} d_{21} e^{-\alpha_1 (2d-|z-z_k|)} \end{array}}{s_{10} s_{21} - d_{10} d_{21} e^{-2\alpha_1 d}} d\lambda \tag{8}$$

where:

$$s_{10} = \mu_0 \sqrt{\lambda^2 + \frac{j\omega\mu_1}{\rho_1}} + \mu_1 \sqrt{\lambda^2 + j\omega\mu_0\varepsilon_0} \tag{9}$$

$$s_{21} = \mu_2 \sqrt{\lambda^2 + \frac{j\omega\mu_1}{\rho_1}} + \mu_1 \sqrt{\lambda^2 + \frac{j\omega\mu_2}{\rho_2}} \tag{10}$$

$$d_{10} = \mu_0 \sqrt{\lambda^2 + \frac{j\omega\mu_1}{\rho_1}} - \mu_1 \sqrt{\lambda^2 + j\omega\mu_0\varepsilon_0} \tag{11}$$

$$d_{21} = \mu_2 \sqrt{\lambda^2 + \frac{j\omega\mu_1}{\rho_1}} - \mu_1 \sqrt{\lambda^2 + \frac{j\omega\mu_2}{\rho_2}} \tag{12}$$

$$\alpha_1 = \sqrt{\lambda^2 + \frac{j\omega\mu_1}{\rho_1}} \tag{13}$$

μ_1 and μ_2 being the magnetic permeability of sea water and seabed, respectively, and ε_0 the vacuum dielectric permittivity.

3. FORMULAS FOR THE SHIELDING FACTOR

3.1. General

The phase conductors inside a submarine power cable are, in many cases, contained inside a tubular lead or aluminium sheath. In turn, the sheath is helicoidally wrapped by means of a certain number of steel wires constituting the cable armouring which has purposes of mechanical protection.

Both sheath and armouring are important from the electromagnetic point of view because they shield the EMF which is primarily produced by the current flowing in the phase conductors; thus, a correct evaluation of the EMF generated by the power cable should take into account of the shielding effect related to sheath and armouring.

In this paragraph, we want to give expressions for the shielding factor S (or shielding effectiveness) of a tubular sheath and of an armouring in function of their physical and geometrical characteristics.

The screening factor is generally defined as:

$$S = \frac{|B_{\text{with shield}}|}{|B_{\text{without shield}}|} \tag{14}$$

In our case, such a shielding factor can be used also for the electric field because, outside the cable, and it is given by only the inductive component, i.e., the one due to time variations of B field.

The formulas that we are going to present appear in [12, 13], and to those publications we refer for further details.

For the following, two points need to be remarked:

- The formulas for the shielding factor S are valid in points of the space having distances much greater than the distance between the phase conductors; we can notice that such a condition is fulfilled practically everywhere outside the cable.
- In case of two-layer shields, in [13] it is shown that, with good approximation, we have:

$$S \approx S_1 S_2 \tag{15}$$

Formula (15) means that the two shields can be studied separately. Such a principle can be applied to the sheath and to the armouring; thus, the overall cable shielding factor is:

$$S \approx S_{sh} S_{arm} \tag{16}$$

S_{sh} and S_{arm} being the shielding factors associated to the cable sheath and armouring, respectively.

3.2. Shielding Factor of the Sheath

Let us define by δ_{sh} the skin depth relevant to the metal composing the sheath given by:

$$\delta_{sh} = \sqrt{\frac{\rho_{sh}}{\pi f \mu_0 \mu_{r\,sh}}} \tag{17}$$

ρ_{sh} and $\mu_{r\,sh}$ being the sheath resistivity and relative magnetic permeability, respectively.

The shielding factor relevant to the sheath of inner radius R_{sh} and thickness t_{sh} is:

$$S_{sh} = \frac{\sqrt{2}\,\frac{\mu_{r\,sh}\delta_{sh}}{R_{sh}+t_{sh}}}{\left|1-0.5j\left(\frac{\mu_{r\,sh}\delta_{sh}}{R_{sh}+t_{sh}}\right)^2 \sinh\left[\frac{t_{sh}}{\delta_{sh}}(1+j)\right]+(1-j)\,\frac{\mu_{r\,sh}\delta_{sh}}{R_{sh}+t_{sh}}\cosh\left[\frac{t_{sh}}{\delta_{sh}}(1+j)\right]\right|} \tag{18}$$

3.3. Shielding Factor of the Armouring

As already mentioned, the armouring is formed by n steel wires, having radius r_w and resistivity ρ_{arm}, helicoidally wrapped around the sheath with pitch p and laying angle ψ (see Figure 3).

By following the ideas and using the information given in [14], the armouring can be reduced to an equivalent tubular conductor.

The equivalent thickness of the armouring is given by:

$$t_{arm} = \sqrt{R_{arm}^2 + n r_w^2 \cos(\psi)} - R_{arm} \tag{19}$$

where R_{arm} is the inner radius of the armouring.

As far as the steel wires relative permeability is concerned, as shown in [14], we have it split up into two different components (see Figure 3):

- A longitudinal component (i.e., in the direction of the wires) $\mu_{rl} = |\mu_{rl}|e^{-j\alpha}$ which is represented by a complex number in order to take into account of eddy current and hysteresis losses inside steel wires.
- A transversal component (i.e., in the direction normal to the wires) μ_{rt}.

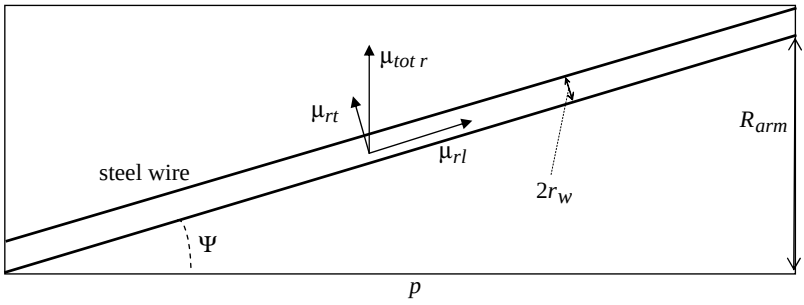

Figure 3. Geometrical and physical parameters associated to armouring steel wires.

The values of both longitudinal and transversal relative permeabilities are function of magnetic field and depend also on other parameters such as steel wires diameter and tensile strength. In [14], some experimental curves are reported.

Next step, in transforming the steel wire armouring into an equivalent tubular conductor, is the introduction of an equivalent total relative permeability μ_{rtot} given by:

$$\mu_{r\,tot} = \frac{\pi n r_w}{2p} \left|\mu_{rl}\right| e^{-j\alpha} \sin\psi + \mu_{rt} \cos^2\psi \tag{20}$$

Even if $|\mu_{rl}|$, α and μ_{rt} depend on magnetic field intensity, representative values for them, for different values of wire diameter, are given in Table 1.

Therefore, formula (20) allows us to calculate an equivalent value of armouring magnetic relative permeability; then, by considering $|\mu_{r\,tot}|$ and by means of analogous formulas to (17) and (18) the

Table 1. Representative values for some armouring steel wires parameters; $f = 50\,\text{Hz}$, tensile strength 600–700 MN/m^2.

wires diameter [mm]	$\lvert\mu_{rl}\rvert$	α [deg]	μ_{rt}
5	400	52	10 for wires in contact 1 for separated wires
3.25	600	49	10 for wires in contact 1 for separated wires
2	700	40	10 for wires in contact 1 for separated wires

shielding factor associated to armouring itself can be estimated, i.e.,

$$S_{arm} = \frac{\sqrt{2}\frac{\mu_{rtot}\delta_{arm}}{R_{arm}+t_{arm}}}{\left|1 - 0.5j\left(\frac{\mu_{rtot}\delta_{arm}}{R_{arm}+t_{arm}}\right)^2 \sinh\left[\frac{t_{arm}}{\delta_{arm}}(1+j)\right] + (1-j)\frac{\mu_{rtot}\delta_{arm}}{R_{arm}+t_{arm}}\cosh\left[\frac{t_{arm}}{\delta_{arm}}(1+j)\right]\right|} \quad (21)$$

4. A COMPARISON WITH DIFFERENT EXISTING MODELS

In this paragraph, we present a comparison among the results obtained by using FEM, radial transmission line method, infinite sea model (according to Section 2.2) and finite depth sea model (according to Section 2.3). The data and results concerning the first two methods have been reported in [10].

A single phase AC (60 Hz) shielded cable carrying a current of 1 A (RMS) and submerged in an infinite sea (having $\rho_1 = 0.25\,\Omega$m) has been considered. The peak values of electric and magnetic field versus the radial distance from the cable axis calculated according to the above mentioned four different models are shown in Table 2 and Table 3.

The results in Table 2 and Table 3 show an overall and fair agreement for the electric field and a good agreement for the magnetic flux density fields. It is also necessary to mention that the results relevant to the first three methods (columns 2–4) have been obtained under the assumption of infinite sea model while the results in column 5

Table 2. Electric field versus radial distance calculated according to four different models.

Distance from cable axis [m]	FEM [μV/m]	Radial transmission line model [μV/m]	Analytical-infinite sea model [μV/m]	Analytical-finite depth sea model; (with $\rho_2 = 1\,\Omega$m, $d = 10$ m) [μV/m]
0.1	190.8	202	199.3	220.5
0.2	165.8	178	175	196.4
0.5	132.5	145	142.9	164.6
1	107.7	121	118.8	140.7
2	82.5	96	95.1	117.3
5	49.5	65	64.5	87.6
10	24.7	43	42.8	66.7

Table 3. Magnetic flux density field versus radial distance calculated according to four different models.

Distance from cable axis [m]	FEM [μT]	Radial transmission line model [μT]	Analytical-infinite sea model [μT]	Analytical-finite depth sea model; (with $\rho_2 = 1\,\Omega$m, $d = 10$ m) [μT]
0.1	0.946	0.957	0.943	0.926
0.2	0.480	0.478	0.471	0.471
0.5	0.191	0.191	0.189	0.189
1	0.097	0.096	0.094	0.094
2	0.048	0.048	0.047	0.047
5	0.019	0.019	0.019	0.018
10	0.0096	0.009	0.009	0.008

have been obtained by using a finite depth sea model, which explains the differences with respect to the other methods (see also the results in the next paragraph).

5. COMPARISON BETWEEN THE TWO DIFFERENT ANALYTICAL CALCULATION MODELS

This section is devoted to present the comparison among the results obtained by applying the different analytical EMF expressions introduced in Section 2. At first, it is necessary to remark that the two analytical models, previously introduced, are now applied by considering more than one conductor. In fact, a typical submarine power cable is composed by its three phase conductors carrying a known constant and balanced current. In this case, the total field is obtained by means of the superposition principle by adding the three single contributions through the expressions given in Section 2. The other conductors present in the cable, i.e., metallic sheath and armouring, are coupled with the phase conductors and offer an important shielding effect, and their presence is taken into account by means of suitable shielding factors that have been described in Section 3.

So, in order to have an idea of the performance offered by the two different models in relation to the main physical and geometrical parameters involved in the models, it is convenient to introduce the per cent relative difference between the modulus of the field evaluated according to the infinite sea model and finite depth sea model for both

electric and magnetic fields, i.e.,

$$eE_{\%}(y,z) = \frac{|E(y,z)| - |E'(y,z)|}{|E'(y,z)|}100 \tag{22}$$

$$eB_{\%}(y,z) = \frac{|B(y,z)| - |B'(y,z)|}{|B'(y,z)|}100 \tag{23}$$

It is evident that a very important parameter is the sea water resistivity ρ_1, which depends on the water salinity and temperature and typically ranges in the interval $[0.25,\ 2]\,\Omega$m. Other minor parameters are: the seabed resistivity ρ_2, the laying depth d.

In the calculations, we shall consider a single core 132 kV–50 Hz tri-phase submarine cable with trefoil disposition of the conductors and carrying a balanced current of 700 A: the distance among them is 72 mm and the shielding factor associated to the sheath and armouring is $S = 0.5$.

The phase conductors coordinates and relevant currents are given in Table 4.

Table 4. Cable conductors coordinates and relevant currents.

conductor	y [m]	z [m]	Current modulus [A]	Current phase
C	-0.036	0.036	700	120°
B	0	0.062	700	240°
A	0.036	0.036	700	0°

Figures 4 and 5 show, on the primary ordinate axis (on the left and in logarithmic scale), the modulus of electric and magnetic flux density field versus lateral distance from the cable evaluated at $z = 1$ m, from the seabed level, for different values of sea water resistivity. On secondary axis (on the right) the relevant per cent relative difference between the results obtained by the two models is shown.

Figures 6 and 7 show, on the primary ordinate axis (on the left and in logarithmic scale), the modulus of electric and magnetic flux density field versus lateral distance from the cable for two different values of the seabed resistivity. In particular, the value $\rho_2 = 5\,\Omega$m corresponds to a seabed mainly composed by sediments while the value $\rho_2 = 1000\,\Omega$m corresponds to a rocky seabed. On secondary axis (on the right) the relevant per cent relative difference between the results obtained by the two models is shown. The calculations have been performed for two different heights with respect to the seabed level, i.e., $z = 0.5$ m and $z = 5$ m.

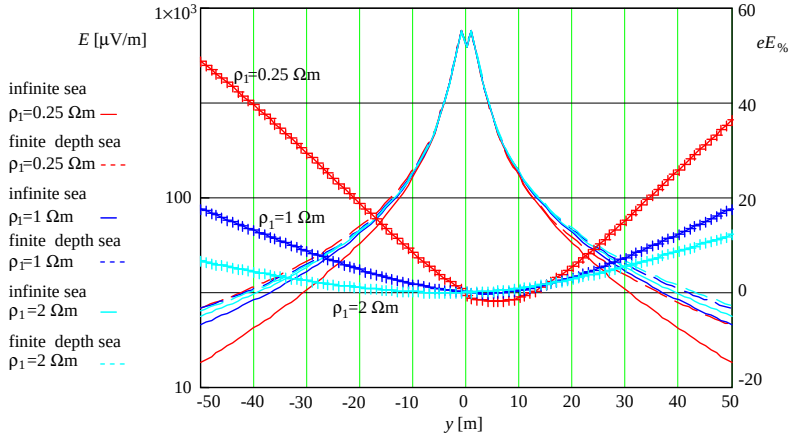

Figure 4. Electric field (primary ordinate axis) and per cent relative difference (secondary ordinate axis) versus lateral distance from the cable evaluated for different values of sea water resistivity; $z = 1\,\text{m}$, seabed resistivity $\rho_2 = 5\,\Omega\text{m}$, laying depth $d = 10\,\text{m}$.

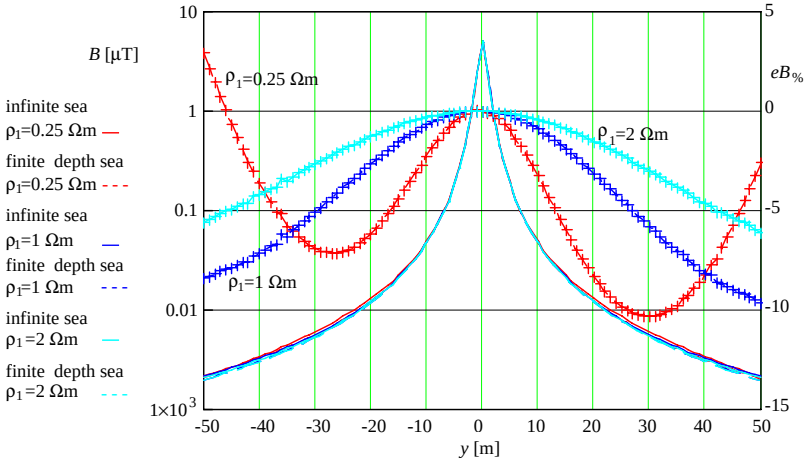

Figure 5. Magnetic flux density field (primary ordinate axis) and per cent relative difference (secondary ordinate axis) versus lateral distance from the cable evaluated for different values of sea water resistivity; $z = 1\,\text{m}$, seabed resistivity $\rho_2 = 5\,\Omega\text{m}$, laying depth $d = 10\,\text{m}$.

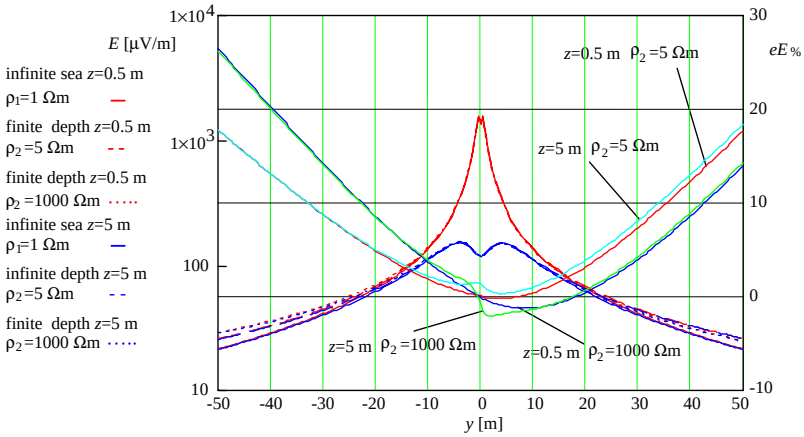

Figure 6. Electric field (primary ordinate axis) and per cent relative difference (secondary ordinate axis) versus lateral distance from the cable evaluated for different heights from seabed and different seabed resistivity; sea water resistivity $\rho_1 = 1\,\Omega$m, laying depth $d = 10\,$m.

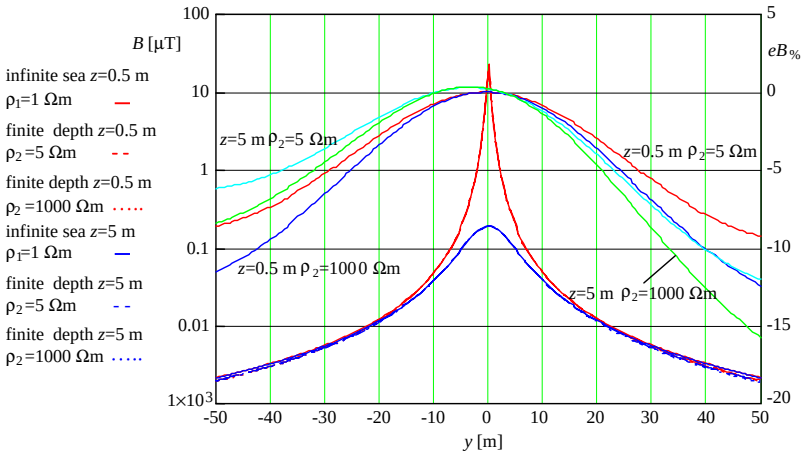

Figure 7. Magnetic flux density field (primary ordinate axis) and per cent relative difference (secondary ordinate axis) versus lateral distance from the cable evaluated for different heights from seabed and different seabed resistivity; sea water resistivity $\rho_1 = 1\,\Omega$m, laying depth $d = 10\,$m.

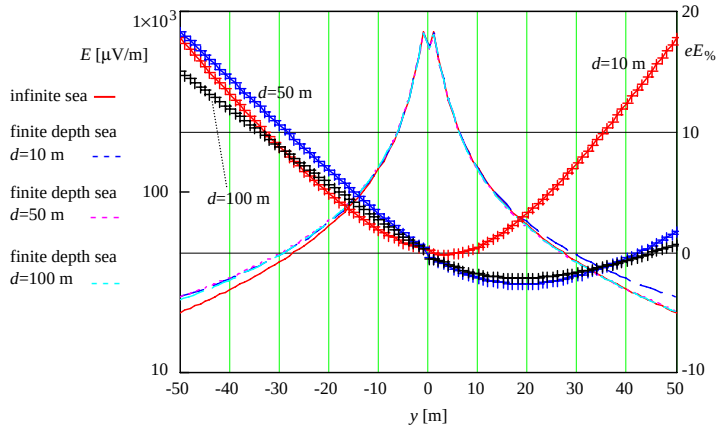

Figure 8. Electric field (primary ordinate axis) and per cent relative difference (secondary ordinate axis) versus lateral distance from the cable evaluated for different laying depths; sea water resistivity $\rho_1 = 1\,\Omega$m, seabed resistivity $\rho_2 = 5\,\Omega$m, $z = 1$ m.

Figures 8 and 9 show, on the primary ordinate axis (on the left and in logarithmic scale), the modulus of electric and magnetic flux density field versus lateral distance from the cable by considering different values for laying depth of the cable (or, equivalently, of the sea depth), i.e., $d = 10$ m, $d = 50$ m, $d = 100$ m. On secondary axis (on the right) the relevant per cent relative difference between the results obtained by the two models is shown. Values for ρ_1 and ρ_2 are $1\,\Omega$m and $5\,\Omega$m, respectively. The calculations have been performed at height $z = 1$ m from the seabed level.

By looking at Figures 4–9 we can do the following remarks:

1. EMF very rapidly decays with the distance from the cable.
2. All the cases studied show small differences between the infinite sea model and the finite depth sea model in the regions near to the cable, but, by increasing the distance from the cable itself, the deviations between the results of the two models increase. Such kind of trend is more pronounced for the electric field than for the magnetic flux density field.
3. When the cable laying depth (or equivalently the sea depth) increases, the discrepancies between the two models decrease, which is intuitive because as the layer of sea water above the cable increases, it tends to be more similar to an infinite thickness layer. So, in case of shallow water, (typically close to the shore) it is better to use the finite depth sea model.

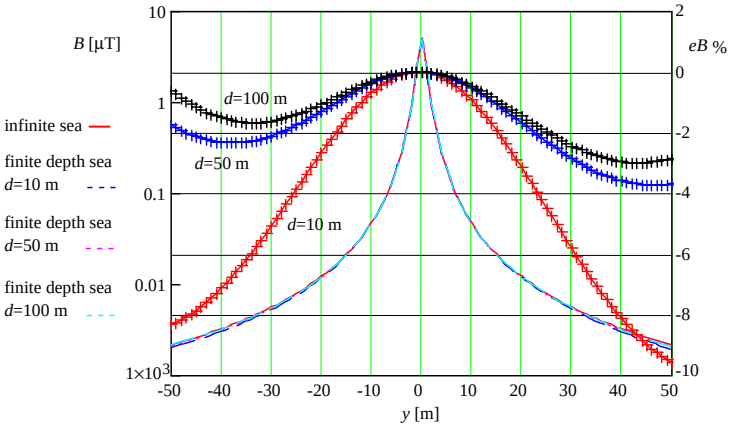

Figure 9. Magnetic flux density field (primary ordinate axis) and per cent relative difference (secondary ordinate axis) versus lateral distance from the cable evaluated for different laying depth; sea water resistivity $\rho_1 = 1\,\Omega$m, seabed resistivity $\rho_2 = 5\,\Omega$m, $z = 1$ m.

On the whole, we can conclude that the two models give consistent results.

6. CONCLUSIONS

In the frame of the environmental impact assessment of offshore wind farms, we have presented and compared two different analytical models for the calculation of ELF sub-sea electromagnetic field produced by submarine power cables.

The two models have also been validated by means of a comparison with FEM and radial transmission line model that gave a fair agreement.

The first and simpler model describes the sea as an infinite, homogeneous and isotropic medium while the second one, proposed in this paper, more realistically, represents the sea as a homogeneous layer of finite thickness between the air and the seabed.

From the comparison of the results relevant to the two models, it appears that small differences exist between them in the regions close to the cable, while, by increasing the distances from it, the deviations between the two models become more significant especially for the electric field.

Thus, the finite depth sea model is a more precise tool to predict the level of under water EMF field generated submarine power cables

especially in points not very close to the cable and/or in case of shallow water; therefore, on the whole, it seems better to use the finite depth model because more general than the infinite sea model.

The paper also gives suitable formulas to take into account of the presence of the cable metallic sheath and armouring which act as shielding structures with respect to the EMF field generated outside the cable.

As a last remark, we notice that both FEM approach and the analytical finite depth sea model are able to study more realistic sea models but the latter is, without any doubt, simpler and can be easily implemented by means of an easy computer program.

REFERENCES

1. Wait, J. R., "Electromagnetic field of current-carrying wires in a conducting medium," *Canadian Journal of Physics*, Vol. 30, 512–523, 1952.
2. Siegel, M. and R. W. P. King, "Radiation from linear antennas in a dissipative half-space," *IEEE Trans. on Antennas and Propagation*, Vol. 19, No. 4, 477–485, Jul. 1971.
3. Kraichman, M. B., *Handbook of Electromagnetic Propagation in Conducting Media,* US Government Printing Office, Washington, DC, 1976.
4. Inan, A. S., A. C. Fraser-Smith, and O. G. Villard, Jr., "ULF/ELF electromagnetic fields produced in a conducting medium of infinite extent by linear current sources of infinite length," *Radio Science*, Vol. 18, No. 6, 1383–1392, 1983.
5. Gill, A. B., I. Gloyne-Phillips, K. J. Neal, and J. A. Kimber, "The potential effects of electromagnetic fields generated by sub-sea power cables associated with offshore wind farm developments on electrically and magnetically sensitive organisms —- A review," COWRIE 1.5, Final Report, Jul. 2005.
6. OSPAR Commission 2008, "Background document on potential problems associated with power cables other than those for oil and gas activities," Publication No. 370, 2008.
7. Ollson, T., A. Larsson, P. Bergsten, and J. Nissen, "Impact of electric and magnetic field from sub-sea cables on marine organisms — The current status of knowledge," Final Report, Vattenfall, Nov. 2010.
8. Gills, A. B., Y. Huang, J. Spencer, and I. Gloyne-Phillips, "Electromagnetic fields emitted by high voltage alternating current offshore wind power cables and interactions with marine

organisms," available at: http://www.theiet.org/communities/electromagnetics/energy-and-power/documents/offshore-wind.cfm?type=pdf.

9. Huang, Y. and I. Gloyne-Phillips, "Electromagnetic simulation of 135 kV three-phase submarine power cables," Report Version 1.2, CMACS (Centre for Marine and Coastal Studies Ltd.), Jul. 2005.
10. Slater, M., R. Jones, and A. Schultz, "The prediction of electromagnetic field generated by submarine power cables," Oregon Wave Energy Trust, Report 0905-00-007, Sep. 2010, available at: http://www.oregonwave.org/wp-content/uploads/7-The-prediction-of-electromagnetic-fields-generated-by-submarine-power-cables.pdf.
11. Tsiamitros, D. A., G. K. Papagiannis, D. P. Labridis, and P. S. Dokopoulos, "Earth return path impedances of underground cables for the two-layer earth case," *IEEE Transactions on Power Delivery*, Vol. 20, No. 3, 2174–2180, 2005.
12. Du, Y. and J. Burnett, "Magnetic shielding principles of linear cylindrical shield at power-frequency," *IEEE 1996 International Symposium on Electromagnetic Compatibility*, 488–493, Santa Clara, California, US, Aug. 19–23, 1996.
13. Du, Y. and J. Burnett, "Optimal magnetic shielding of double-layer shields at power-frequency," *IEEE 1997 International Symposium on Electromagnetic Compatibility*, 191–196, Austin, Texas, US, Aug. 18–22, 1997.
14. Bianchi, G. and G. Luoni, "Induced currents and losses in single-core submarine cables," *IEEE Transactions on Power Apparatus and Systems*, Vol. 95, No. 1, 49–58, 1976.